

HOKKAIDO UNIVERSITY

Title	Aerodynamic scaling for estimating the mean height of dense canopies
Author(s)	Nakai, Taro; Sumida, Akihiro; Matsumoto, Kazuho et al.
Citation	Boundary-Layer Meteorology, 128(3), 423-443 https://doi.org/10.1007/s10546-008-9299-5
Issue Date	2008-09
Doc URL	https://hdl.handle.net/2115/39145
Rights	The original publication is available at www.springerlink.com
Type	journal article
File Information	Nakai_2008BLM_HUSCAP.pdf



Hokkaido University Collection of Scholarly and Academic Papers : HUSCAP

Boundary-Layer Meteorology manuscript No.
(will be inserted by the editor)

Aerodynamic scaling for estimating the mean height of dense canopies

Taro Nakai · Akihiro Sumida · Kazuho Matsumoto · Ken'ichi Daikoku · Shin'ichi Iida · Hotaek Park · Mie Miyahara · Yuji Kodama · Alexander V. Kononov · Trofim C. Maximov · Hironori Yabuki · Toshihiko Hara · Takeshi Ohta

Received: date / Accepted: date

Abstract We used an aerodynamic method to objectively determine the representative canopy height, using standard meteorological measurements. The canopy height may change if the tree height is used to represent the actual canopy, but little work to date has focused on creating a standard for determining the representative canopy height. Here we propose the 'aerodynamic canopy height' h_a as the most effective means of resolving the representative canopy height for all forests. We determined h_a by simple linear regression between zero-plane displacement d and roughness length z_0, without the need

T. Nakai · A. Sumida · Y. Kodama · T. Hara
Institute of Low Temperature Science, Hokkaido University, N19 W8, Kita-Ku, Sapporo 060-0819, Japan
E-mail: taro@pop.lowtem.hokudai.ac.jp, taro.nakai@gmail.com

T. Nakai · T. Ohta
CREST, Japan Science and Technology Agency, Kawaguchi, Saitama 332-0012, Japan

K. Matsumoto
Graduate School of Agricultutural Science, Kyoto University, Kitashirakawa-oiwake-cho, Sakyo-ku, Kyoto 606-8502, Japan

K. K. Daikoku · Mie Miyahara · T. Ohta
Graduate School of Bioagricultural Sciences, Nagoya University, Nagoya 464-8601, Japan

S. Iida
Department of Soil and Water Conservation, Forestry and Forest Products Research Institute, PO Box 16 Tsukuba, Ibaraki 305-8687, Japan

H. Park
Data Integration and Analyses Group, Japan Agency for Marine-Earth Science and Technology, Yokosuka 237-0061, Japan

A. V. Kononov · T. C. Maximov
Institute for Biological Problems of Cryolithozone, Siberian Division of the Russian Academy of Sciences, 41 Lenin ave., Yakutsk 678891, Russia

H. Yabuki
Institute of Observational Research Center for Global Change, Yokosuka 237-0061, Japan

for stand inventory data. The applicability of h_a was confirmed in five different forests, including a forest with a complex canopy structure. Comparison with stand inventory data showed that h_a was almost equivalent to the representative height of trees composing the crown surface if the forest had a simple structure, or to the representative height of taller trees composing the upper canopy in forests with a complex canopy structure. The linear relationship between d and z_0 was explained by assuming that the logarithmic wind profile above the canopy and the exponential wind profile within the canopy were continuous and smooth at canopy height. This was supported by observations, which showed that h_a was essentially the same as the height defined by the inflection point of the vertical profile of wind speed. The applicability of h_a was also verified using data from several previous studies.

Keywords Aerodynamic canopy height · Canopy structure · Roughness length · Zero-plane displacement

1 Introduction

In previous studies of forest micrometeorology, canopy height h (m) was determined using various statistical methods and data often derived from tree heights. Mean tree height was the most commonly used parameter, and some studies determined canopy height as the mean height of a limited number of trees (e.g. Leonard and Federer, 1973; Turnipseed et al., 2002), or approximate mean canopy height (e.g. Viswanadham et al., 1990; Lo, 1995). One difficulty in resolving canopy height is that mean tree height does not always represent the canopy structure of a forest. If a forest is composed of trees with similar heights, the mean tree height may represent the canopy height. However, this is not always the case, other than in even-aged stands, because the mean tree height is much smaller than the expected canopy height in the presence of a large number of shorter trees. For example, in conifer-broadleaf mixed forest in Moshiri, Hokkaido, Japan, although the maximum tree height is 33.6 m, and trees taller than 15 m were 79% of the total basal area (sum of the cross-sectional areas of trunks at breast height (1.3 m)) of the forest, the mean tree height was only 5.1 m (Table 1). Obviously, the mean tree height (5.1 m) is not appropriate for micrometeorological purposes. The canopy height may be defined as the mean tree height for trees composing the upper canopy, but determining which trees compose the upper canopy is still subjective. As for maximum tree height, this also may not be representative of forest height because the tallest tree is often an emergent. Thus far, no standard has been established to determine representative canopy height, especially for forests that have a complex canopy structure. From this perspective, the statistical methods used to determine representative canopy height are not applicable in a general sense, and another approach is required.

Thomas and Foken (2007) defined the 'aerodynamic canopy height' as the height of the inflection point in the vertical profile of the wind speed using a third-order polynomial fitted to measurements at seven heights, which is in

good agreement with a visual estimate for the canopy height. This method was originally suggested by Raupach et al. (1996) and seems reasonable in that it is consistent with the idea that the logarithmic wind profile above the canopy (convex downward) and the exponential wind profile within the canopy (convex upward) are continuous and smooth at canopy height h. However, it might not be applicable to other tower observation sites because it requires wind speed measurements at several heights within and above the forest canopy.

Thom (1971) suggested a linear relationship between roughness length z_0 (m) and zero-plane displacement d (m). This relationship was confirmed by several observations in each particular canopy (e.g. Maki, 1975, 1976; Jacobs and van Boxel, 1988). Based on this relationship, Maki (1975, 1976) defined the 'effective plant height', which can be obtained from this linear relationship. In general, because both d and z_0 can be obtained from most micrometeorological towers, this method is likely suitable for determining the canopy height of a forest. However, no other studies using Maki's effective plant height were found in the literature, and the canopies that Maki (1975, 1976) investigated were composed of a single species with almost homogeneous plant heights; thus, the applicability of Maki's effective plant height to forests with complex canopy structure is still unknown. Furthermore, the correspondence between this height and the actual distribution of tree heights within a stand has not been surveyed.

Our objective was to explore the possible use of aerodynamic height as a representative canopy height scale for biosphere-atmosphere mass, energy and momentum exchange studies. As the most effective means, we introduce Maki's effective plant height as the 'aerodynamic canopy height' and discuss the characteristics and applicability of this height by applying it to five different forests, including those with complex canopy structure, and compare the results with stand inventory data. The consistency of the aerodynamic canopy height introduced here and that defined by Thomas and Foken (2007) is also discussed.

2 Theoretical aspects of the aerodynamic canopy height

In this section, we demonstrate a theoretical linear relationship between d and z_0 (Thom, 1971) and define the physical meaning of the aerodynamic canopy height. We consider a dense canopy only because the exponential mean velocity profile within the canopy (Inoue, 1963) introduced below is valid only in dense conditions.

We consider the case in which the vertical profile of the wind speed above the canopy ($z \geq h$, where z (m) is the height from the ground) follows the logarithmic law:

$$U = \frac{u_*}{k} \ln \frac{z-d}{z_0}, \tag{1}$$

and the flow within the canopy ($z \leq h$) follows the exponential law (Inoue, 1963):

$$U = U_{\mathrm{h}} \exp[\gamma(z - h)], \tag{2}$$

where U_{h} is the wind speed at $z = h$, and γ (m^{-1}) is the coefficient of momentum absorption, defined as

$$\gamma = \left(\frac{a c_{\mathrm{d}}}{2 l_{\mathrm{h}}^2} \right)^{1/3}, \tag{3}$$

where a ($\mathrm{m}^2\ \mathrm{m}^{-3}$) is the leaf area density, c_{d} (dimensionless) is the drag coefficient, and l_{h} (m) is the mixing length at the top of the canopy, $z = h$. When deriving Eqs. (2) and (3), Inoue (1963) assumed that l_{h} and ac_{d} are constant within the canopy layer.

If Eqs. (1) and (2) are continuous and smooth for $z = h$, the derivatives of these equations at $z = h$ are equal. The derivatives of Eqs. (1) and (2) are

$$\frac{\mathrm{d}U}{\mathrm{d}z} = \frac{u_*}{k(z - d)}, \qquad z \geq h, \tag{4}$$

and

$$\frac{\mathrm{d}U}{\mathrm{d}z} = \gamma U_{\mathrm{h}} \exp[\gamma(z - h)], \qquad z \leq h \tag{5}$$

respectively. These are combined at $z = h$ as follows:

$$\frac{u_*}{k(h - d)} = \gamma U_{\mathrm{h}}. \tag{6}$$

Substituting Eq. (1) into Eq. (6) for $z = h$ results in

$$\ln \frac{h - d}{z_0} = \frac{1}{\gamma(h - d)}. \tag{7}$$

This equation is the same as that derived by Kondo (1971), assuming continuity of the friction velocity u_* at $z = h$ (see Appendix A). Considering the continuity in the shear stress, our theoretical result and the theory of Kondo (1971) summarised in Appendix A are essentially equal (see Appendix B).

Because γ represents the momentum absorption by the leaves, and $h - d$ is the depth proportional to the length in which the downward momentum disappears, $\gamma(h - d)$ is assumed to be a non-dimensional constant (Kondo, 1971). Therefore, this result theoretically supports the linear relationship between $h - d$ and z_0, which was suggested by Thom (1971) to be

$$z_0 = \lambda(h - d), \tag{8}$$

where λ (dimensionless) is a constant specific to a stand. The values of λ and the canopy height specific to a forest h_{a} ($= d + z_0/\lambda$) (m) can be determined by regression using Eq. (8) and the observed values of d and z_0. Thom (1971) determined that $\lambda = 0.36$, calculated from the relationships $d = 0.64h$ (Cowan, 1968) and $z_0 = 0.13h$ (Tanner and Pelton, 1960). Maki (1975, 1976) called this

h_a 'effective plant height'. Hereafter, we refer to h_a as the 'aerodynamic canopy height' to clarify the derivation and meaning of this parameter.

The above theory demonstrates that the linear relationship between $h - d$ and z_0 is equivalent to an assumption that the logarithmic wind profile above the canopy and the exponential wind profile within the canopy are continuous at canopy height $z = h$. This indicates that the aerodynamic canopy height h_a derived from Eq. (8) is essentially the same as that derived from the height of the inflection point in the vertical wind profile (Thomas and Foken, 2007). In Section 5.1, we confirm the consistency of these two definitions using observational data.

3 Observations

3.1 Study sites

We applied this method to a larch forest (YL) and a pine forest (YP) in Spasskaya Pad, near Yakutsk, Russia; a birch forest (MB) and a conifer-deciduous broadleaf mixed forest (MM) in Moshiri, Japan; and an evergreen-deciduous broadleaf mixed forest (SM) in Seto, Japan (Table 1, Fig. 1). The location, altitude (m), stand density (stands ha^{-1}), maximum tree height h_{max} (m), mean tree height h_m (m) and standard deviation of tree heights σ_h (m) at these forest sites are listed in Table 1.

3.2 Meteorological observations

To obtain d and z_0, we used two wind speeds U_1 and U_2 (m s^{-1}) at two heights z_1 and z_2 (m), measured using cup anemometers, and friction velocity, u_* (m s^{-1}) at z_e (m), measured using an ultrasonic anemometer. The cup anemometers used were AC-750 (Makino, Japan) at sites YL and YP, and 010C (MetOne, USA) at sites MB, MM and SM. The ultrasonic anemometers R3-50 Solent (Gill Instruments, UK) were used at sites YL, YP, MB and MM, and DAT-540 (Kaijo, Japan) was used at site SM. U_1 and U_2 were sampled at 10-s intervals and averaged over 30 min, and u_* was calculated every 30 min from wind speed data sampled at a rate of 10 Hz. For R3-50, angle-of-attack-dependent errors were corrected in calculating u_* (Nakai et al., 2006). Measurement heights z_e, z_1 and z_2 of observation sites are shown in Table 1. Although the maximum tree height of site MM was greater than the measurement height, the tallest tree was located downslope and distant from the tower. The tree heights near the tower were short enough for the instruments to be located above the canopy.

From these measurements, d and z_0 under neutral conditions were calculated as follows (e.g. Rooney, 2001; Nakai et al., 2005, 2008):

$$d = \frac{z_2 \exp(kU_1/u_*)/\exp(kU_2/u_*) - z_1}{\exp(kU_1/u_*)/\exp(kU_2/u_*) - 1}, \tag{9}$$

$$z_0 = \frac{z_1 - d}{\exp(kU_1/u_*)}, \tag{10}$$

where k (dimensionless) is the von Kármán constant. The data under the condition of neutral stability ($|z_e/L| < 0.05$, where L (m) is the Obukhov length) and $u_* \geq 0.5$ in summer (JJA) 2004 (YL, YP), 2005 (MB, MM) and 2006 (SM), were used for this calculation. Furthermore, the data used were limited by the range of wind directions (Table 1) to avoid the shadow effect of the tower.

3.3 Forest survey

To compare the estimated aerodynamic canopy height h_a with stand inventory data, forest surveys were conducted in 2003 (YL, YP, MB), 2004 (YL, YP, MM), 2005 (SM) and 2006 (YP; Table 1). The tree height h_i (m), basal area of each tree A_i (m^2) and number of trees N were measured at all of the forest sites (where the subscript i indicates tree number). Mean tree height $h_m = (1/N)\sum h_i$, maximum tree height h_{max} and the standard deviations σ_h (Table 1) were obtained from these data. In addition, weighted mean canopy height with a basal area $h_B = \sum (h_i A_i) / \sum A_i$ (m) was also calculated and is referred to in the next section.

To consider the vertical structure of a forest, the frequencies of tree height and basal area of trees in each 1-m tree height class were calculated. These were normalised using the total number of trees and total basal area to express them in terms of the probability density.

4 Results

Linear relationships between d and z_0 occurred for all five forest sites (Figure 2). To obtain h_a from these plots, we used the geometric mean regression model (Model II), which minimises both the vertical and horizontal residuals (e.g. Riggs et al., 1978; Zobitz et al., 2006). Figure 2 also shows the regressions using the Model II method. The coefficients for λ in Eq. (8) of these sites, calculated from the Model II regression, were 0.26 (YL), 0.27 (YP), 0.26 (MB), 0.37 (MM) and 0.36 (SM). These values are consistent with the estimated λ in previous studies (Table 2). From these regressions, the aerodynamic canopy height h_a of each forest was estimated as 18.4 m (YL), 9.2 m (YP), 11.8 m (MB), 24.3 m (MM) and 8.4 m (SM).

Figure 3 shows a comparison of aerodynamic canopy height h_a with various values calculated from stand inventory data (see section 3.3). In the right-hand figures, the gently sloping part of the cumulative height-frequency curve shows that several trees were within a similar height class. The patterns of the curves were quite different among sites. MB had an upward convex curve corresponding to the presence of many taller trees, whereas YP had two gently sloping parts because of the presence of taller and shorter trees. SM also has

a gently sloping part at approximately 8 m to 10 m. These characteristics also occur in the plot of tree height frequency distributions (grey bars in the middle figures in Fig. 3) as monomodal distributions in MB and SM and bimodal distribution in YP. However, YL had a monotonically decreasing pattern in the curve of cumulative height-frequency probability, and correspondingly, no distinct peaks in the tree height frequency distributions were found. In the case of site MM, the cumulative height-frequency curve had a downward convex curve because the fraction of taller trees was quite small and the distribution of tree height frequencies was extremely slanted toward shorter trees.

The aerodynamic canopy height h_a corresponded to the (upper) peak of the tree height frequency distributions at sites YP, MB and SM, which were almost equivalent to the height of the gently sloping part of the cumulative height-frequency curve because of the presence of trees with corresponding heights. These data indicate that h_a is equivalent to the representative height of trees composing the crown surface if many trees occur within a similar height class.

The h_a was also in agreement with the distribution peak of the basal areas of trees belonging to each 1-m tree height class (open bars in the figures in the middle section of Fig. 3) at all sites, although the peak for site MM was unclear. Because the crown projection area of a tree is reported to increase with individual basal area or DBH (e.g. Shimano, 1997), the upper canopy portion of a forest, which has an effect on the wind profile, would be mainly composed of taller trees with large basal areas. Therefore, h_a would be regarded as the representative height of the taller trees composing the upper canopy.

The mean tree height h_m was smaller than h_a, that is, h_m underestimated the representative canopy height, especially at site MM. These differences resulted from the complex architectures of the forests, as described earlier. Although some previous studies used the mean height of a few of the taller trees as representative of canopy height, the threshold for taller trees is not standardised. For example, the number (or proportion) of taller trees or the DBH was used as the threshold for the averaging procedure, but h_a was equivalent to the mean height of the samples taller than 67.8 (YL), 50.5 (YP), 47.1 (MB), 3.8 (MM), and 96.5% (SM) or the mean tree height of samples with DBH exceeding 14.0 (YL), 7.3 (YP), 8.4 (MB), 37.7 (MM), and 4.1 (SM) cm. Therefore, the statistical methods used previously necessarily involve uncertainty.

By contrast, h_a was similar to the weighted mean canopy height with basal area of h_B at sites YL, YP, and MB. This suggests that h_B also represents canopy height when the canopy structure is relatively simple. However, h_B was 2.7 m smaller than h_a in MM, where the canopy structure was complex. Considering this uncertainty, h_a is more suitable than h_B to represent canopy height in different types of forest for micrometeorological purposes.

In the case of site SM, however, h_B was larger than h_a. At this site, the meteorological tower was located on a mountain ridge, and relatively tall trees were located downslope (Fig. 4). These tall trees were reflected in the results of the forest survey (Fig. 3). The maximum and mean tree heights near the tower (within a 10×10 m plot) were 10.7 and 7.9 m, respectively. The h_a was

based on measurements from the meteorological tower and thus represents the height from the base of the tower to the representative crown surface. In fact, trees around the tower formed the crown surface, and h_a appeared to represent the height of this surface. Considering these conditions, h_a can be regarded as the representative height of the crown surface, with its origin at the base of the tower.

5 Discussion

5.1 Comparison with the aerodynamic canopy height of Thomas and Foken (2007)

The aerodynamic canopy height h_a used here is different from that defined by Thomas and Foken (2007), but the theoretical development in section 2 suggests that these definitions are essentially the same. To confirm this consistency, the definition by Thomas and Foken (2007) was applied to the observed data at sites MB, MM and SM, where wind speeds were observed at five (MB, MM) and six heights (SM). Wind speeds at each height were normalised to the wind speed at the top of the tower. Because the number of measurement heights at these sites was less than that in Thomas and Foken (2007) (seven heights), the results of a third-order polynomial fit seemed unrealistic. Thus, cubic spline interpolation was applied to the vertical profile of the mean relative wind speeds.

Figure 5 shows the vertical profile of the mean relative wind speeds, with their standard deviations, and the vertical mean relative wind speed profiles obtained by cubic spline interpolation for sites MB, MM and SM. The inflection points of these cubic spline functions and our results for h_a are also indicated in the figure. At site MB, the inflection point was close to our h_a, suggesting that the canopy heights obtained from both definitions are essentially the same. However, the inflection points of sites MM and SM were 7.4% and 17.3% higher, respectively, than h_a. This may have occurred because the inflection point was variable at sites MM and SM, as suggested by the fact that the standard deviations of the relative wind speed at sites MM and SM were larger than for site MB. Moreover, the wind profiles of our sites were fitted by cubic spline curves through the data points, whereas Thomas and Foken (2007) determined this from a third-order polynomial curve using a least-square fit that might not pass through the data point. Considering these uncertainties, the aerodynamic canopy height h_a introduced here appears identical to that defined by Thomas and Foken (2007), as theoretically demonstrated in section 2.

Applying a cubic spline interpolation to the vertical profile of the mean wind speed at sites MB, MM, and SM, the shear length scale L_s was estimated as follows (Raupach et al., 1996; Brunet and Irvine, 2000):

$$L_s = \frac{U_{h_a}}{(\mathrm{d}U/\mathrm{d}z)_{z=h_a}}, \tag{11}$$

where U_{h_a} and $(\mathrm{d}U/\mathrm{d}z)_{z=h_a}$ are the mean wind speed and vertical gradient of wind speed at the aerodynamic canopy height h_a, respectively. The normalised L_s/h_a of sites MB, MM, and SM was 0.44, 0.41, and 0.30, respectively. These values were consistent with the findings of Brunet and Irvine (2000) that L_s/h varied between 0.3 and 0.5 in near-neutral conditions.

5.2 Application to other data in the literature

Table 3 shows canopy height h, zero-plane displacement d and roughness length z_0 taken from previous studies. From these data, the coefficient λ was calculated as $\lambda = z_0/(h-d)$. Calculated λ ranged from 0.11 to 0.54 (Table 3), with an average of 0.32 and a standard deviation of 0.12. The aerodynamic canopy height h_a was estimated assuming $\lambda = 0.32 \pm 0.12$. Although the canopy heights in previous studies were determined using various methods, they were well reproduced by the aerodynamic canopy height h_a. If λ of each forest was determined by linear regression of d and z_0 using more data, a reliable h_a would be obtained. Previous statistical methods used in the literature involved uncertainty, as pointed out in section 4; thus, in general, it is difficult to adopt an adequate method to determine the representative canopy height of these forests. The results shown above indicate that the aerodynamic canopy height h_a would be applicable not only to our sites, but also to other forests. Therefore, the aerodynamic canopy height h_a would be appropriate as a general representation of the canopy height of a forest.

5.3 Issues in applying this method

5.3.1 Roughness sublayer problem

It has been pointed out that the roughness sublayer exists immediately above the forest, where the Monin-Obukhov similarity theory fails, and thus, the observed wind profile deviates from the logarithmic low. Because the measurement levels of our sites might be within the roughness sublayer, the effect of the roughness sublayer on the wind speed distribution should be considered. To correct the deviation of the wind speed distribution from the logarithmic low, a number of roughness sublayer functions have been proposed (e.g. Garratt, 1980; Raupach, 1992, 1994; Cellier and Brunet, 1992; Mölder et al., 1999). In applying these functions, it is necessary to know the height of the roughness sublayer z_* (m). To estimate z_*, measurements of wind speed at several heights within and above the roughness sublayer are required. However, such profile measurements were not available at our sites, so reliable correction of the roughness sublayer could not be applied. Therefore, we assessed the effect of roughness sublayer correction on aerodynamic canopy height using a simple simulation.

According to Mölder et al. (1999), d and z_0 under neutral conditions (Eqs. (9) and (10)) are corrected as follows:

$$d = \frac{z_2 \dfrac{\exp(kU_1/u_* - \Psi_\mathrm{u}(z_1))}{\exp(kU_2/u_* - \Psi_\mathrm{u}(z_2))} - z_1}{\dfrac{\exp(kU_1/u_* - \Psi_\mathrm{u}(z_1))}{\exp(kU_2/u_* - \Psi_\mathrm{u}(z_2))} - 1}, \tag{12}$$

$$z_0 = \frac{z_1 - d}{\exp(kU_1/u_* - \Psi_\mathrm{u}(z_1))}, \tag{13}$$

where $\Psi_\mathrm{u}(z)$ is the integrated roughness sublayer function derived as:

$$\begin{aligned}\Psi_\mathrm{u}(z) &= \int_z^{z_*} \frac{1 - [(z' - d)/(z_* - d)]^n}{z' - d} \mathrm{d}z' \\ &= -\ln\left(\frac{z - d}{z_* - d}\right) + \frac{1}{n}\left[\left(\frac{z - d}{z_* - d}\right)^n - 1\right],\end{aligned} \tag{14}$$

where n is the coefficient. Mölder et al. (1999) provided $n = 0.6$ for wind speed correction over a boreal forest (mixed forest of spruce and pine).

From Mölder et al. (1999), z_* for momentum was approximately 1.84 times the maximum tree height. Thus, we assumed $z_* = 1.85h_\mathrm{a}$, where h_a is the aerodynamic canopy height evaluated without roughness sublayer correction. The assumed z_* for our forest sites were 34.0 (YL), 17.0 (YP), 21.9 (MB), 45.0 (MM) and 15.5 m (SM), respectively. In these cases, the upper measurement level of wind speed, z_1, was within the roughness sublayer in sites YL, MB, MM and SM, but close to z_* in sites YL, MB and SM. Furthermore, d is required in calculating $\Psi_\mathrm{u}(z)$; thus, the mean value of d without roughness sublayer correction was used. Using these z_* and d, the aerodynamic canopy height was corrected to 18.9 (YL), 9.4 (YP), 12.4 (MB), 25.0 (MM) and 8.7m (SM). These results were slightly larger than the uncorrected h_a by 0.2 – 0.7 m, equivalent to the increment of 2.2 – 5.1% of h_a. From these results, an expected estimation error of h_a with respect to roughness sublayer correction would be at most several percent.

Recently, Harman and Finnigan (2007) proposed an alternative parameterisation of $\Psi_\mathrm{u}(z)$ that does not use the roughness sublayer height z_*. Under neutral conditions, $\Psi_\mathrm{u}(z)$ is written as follows:

$$\Psi_\mathrm{u}(z) = \int_z^{\infty} \frac{c_1 \exp\{-\beta c_2 (z' - d)/l_\mathrm{h}\}}{z' - d} \mathrm{d}z', \tag{15}$$

where c_1 and c_2 are constants, $\beta = u_*/U_\mathrm{h}$, and $l_\mathrm{h} = 2\beta^3/(ac_\mathrm{d})$ (see Appendix B). In deriving $\Psi_\mathrm{u}(z)$ from Eq. (15) by numerical integration, we took $c_\mathrm{d} = 0.25$, $c_1 = (1 - k/(2\beta))\exp(c_2/2)$ and $c_2 = 0.2$ according to Harman and Finnigan (2007), and assumed $a = A/(0.5h)$ for pure stands (YL, YP, MB) and $a = A/h$ for mixed forests (MM, SM), where A ($\mathrm{m^2\ m^{-2}}$) represents the plant area index in summer (JJA) measured by a plant canopy analyser (LAI-2000, LI-COR, Inc., USA) (Nakai et al., 2008). The mean value of d

without roughness sublayer correction was used, as above. The parameter β was determined so as to satisfy the following equation:

$$\exp\left(-\frac{k}{\beta}\right)\exp\left[\Psi_{\mathrm{u}}(h)\right]=\lambda, \tag{16}$$

where the value of λ was determined in Section 4. Since Eqs. (15) and (16) are complementary, these were solved simultaneously by iterating β numerically. From this method, the aerodynamic canopy height h_{a} was corrected to 18.6 (YL), 9.4 (YP), 11.8 (MB), 24.6 (MM) and 8.6 m (SM). These results were also slightly larger than the uncorrected h_{a} by 0 – 0.3 m, but were closer to the uncorrected h_{a} than to that corrected with Eq. (14).

These assessments indicate that h_{a} can be larger by considering the effect of the roughness sublayer. However, the height of the roughness sublayer z_* is somewhat arbitrary when the detailed wind profile data within and above the roughness sublayer are not available, and d should be the primarily input, which is also arbitrary. The development of the correction method for such conditions is desired, but it is beyond the scope of this study and remains a subject for future investigations.

5.3.2 Method of determining d and z_0

We used wind speeds at two measurement heights to determine d and z_0 via Eqs. (9) and (10) in section 3.2, because wind speeds at just two heights were available for sites YL and YP. However, we measured wind speed at another level z_3 (m) below z_1 and z_2 in sites MB, MM and SM. In these sites, three choices of measurement heights were adopted: the upper pair (z_1, z_2), the lower pair (z_2, z_3) and the pair (z_1, z_3) at either end. Therefore, we checked the sensitivity of the relationship between d and z_0 to the choice of measurement heights.

Figure 6 shows the scatterplot of z_0 against d at sites MB (a), MM (b) and SM (c) calculated from the wind speeds at the upper and lower two heights, at both ends, and at all three heights. The results from the upper two heights were the same as those in Fig. 2. The Model II regression line and resulting h_{a} varied greatly depending on the choice of measurement heights. The slope of the regression line ($=\lambda$) was small for the upper pair, but large for the lower pair. The λ for the both-ends pair was intermediate between them. As a result, h_{a} was underestimated for sites MB and MM when the lower pair or both ends were adopted, while no significant difference in h_{a} was found at site SM. These results showed that h_{a} and the relationship between d and z_0 could vary by the choice of measurement height. From section 5.3.1, we considered all three measurement heights in our sites to be within the roughness sublayer and the deviation of measured wind speed from the logarithmic low to be larger in the lower level. This meant that the sensitivity of the relationship between d and z_0 to the choice of measurement heights would be due to the effect of the roughness sublayer, and the results from the upper two heights adopted in this study were the most reliable in our experimental design.

In most cases, d and z_0 were derived from vertical wind profiles measured at three or more heights (e.g. Monteith and Unsworth, 1990). However, it is recognised that determining d and z_0 from wind profiles is practically difficult since they can vary with measurement uncertainties (e.g. Schaudt, 1998). Figure 7 shows the scatterplot of zero-plane displacement d (Fig. 7a) and roughness length z_0 (Fig. 7b) calculated from the wind profile at three heights against that derived from wind speeds at the upper two heights via Eqs. (9) and (10). The values of d and z_0 calculated from the wind profile varied much more than those calculated using Eqs. (9) and (10). Nevertheless, a clear linear relationship between d and z_0 from the wind profile measured at three heights was found for sites MB, MM and SM (Fig. 6), although the regression line deviated slightly from that derived from the wind speeds at the upper two heights. These deviations were also due to the effect of the roughness sublayer. Thus the linear relationship between d and z_0 demonstrated in section 2 held regardless of the method adopted. Figure 8 shows the scatterplot of friction velocity u_* calculated from the vertical wind profile measured by the cup anemometers at three heights, against that directly measured by the ultrasonic anemometer. Although the u_*-values from the wind profile were larger than those from the ultrasonic anemometer, they were correlated with each other. This indicated that the two measurement types were equivalent, considering the differences in the method of determining u_* and the uncertainty in the measurement of wind speeds at several heights. We therefore judged that the method of determining d and z_0 in this study was adequate.

5.3.3 Limitation of application

It is often reported that roughness length z_0 increases with the density of the roughness element in very sparse canopies, whereas z_0 decreases with density in dense canopies (e.g. Shaw and Pereira, 1982). This indicates that Eq. (8) cannot be balanced for such sparse canopies. Maki (1975, 1976) also showed, using wind tunnel experiments with a canopy composed of glass rods, that h_a underestimated the actual canopy height in sparse canopies. These results suggest a lower limit for the density parameters (such as stand density or plant area index) in applying this method. We could not clarify this limit. Nevertheless, the method investigated here would be applicable to most forests in which micrometeorological observations are carried out.

6 Conclusion

The concept of aerodynamic canopy height h_a was proposed to objectively estimate the representative canopy height of a closed forest. The h_a can be calculated using simple linear regression between zero-plane displacement d and roughness length z_0, without the need for stand inventory data. The applicability of h_a was confirmed in five different forests, including a forest with complex canopy structure. Comparing h_a with stand inventory data, h_a was

almost equivalent to the representative height of trees composing the crown surface if the forest had a simple structure; it can be regarded as the representative height of the taller trees composing the upper canopy in forests with complex canopy structure. This may support the congruence of h_a with actual field data. The applicability of h_a was also suggested from data in the literature.

The linear relationship between d and z_0 was explained by assuming that the logarithmic wind profile above the canopy and the exponential wind profile within the canopy are continuous and smooth at a canopy height $z = h$. This theory also supports the conclusion that the aerodynamic canopy height h_a introduced here is essentially the same as that defined by Thomas and Foken (2007). This consistency of definitions was also confirmed using experimental data from several different forests. A lower limit to the density parameters such as stand density or plant area index would exist when applying this method, but this could not be clarified. Nevertheless, this method would be applicable to most forests in which micrometeorological observations are carried out.

In conclusion, the advantages of aerodynamic canopy height can be summarised as follows:

1. It provides an objective means of determining representative canopy height, whereas previous statistical methods involved uncertainty in the criteria for selecting tree samples.
2. It has the physical meaning of when the logarithmic wind profile above the canopy and the exponential wind profile within the canopy are continuous.
3. It can be determined without the need for stand inventory data, which require extensive field measurements.

Acknowledgements We thank Drs. Takashi Kuwada and Kyoko Kato for providing stand inventory data for Yakutsk (YL, YP) and Moshiri (MB, MM). The topographic data for site SM were obtained with the help of Ms. Yuka Minobe, Mr. Yuji Fujita, Ms. Mari Miyashita, Mr. Kunihiro Katsumata and Ms. Hiroe Takanezawa of Nagoya University, Japan. We also acknowledge the staff members of the Institute for Biological Problems of the Cryolithozone, Siberian Division of the Russian Academy of Sciences, Russia, and Uryu Experimental Forest, Hokkaido University, Japan. Finally, we thank the reviewers of this paper for their valuable comments. This study was conducted as part of the CREST/WECNoF project (P.I.: Takeshi Ohta, Nagoya University, Japan) sponsored by the Core Research for Evolutional Science and Technology (CREST), Japan Science and Technology Agency (JST).

A Theory of Kondo (1971)

Generally, in a horizontally homogeneous canopy, the local change in vertical momentum transfer is related to the drag caused by canopy elements as

$$\frac{1}{\rho}\frac{\mathrm{d}\tau}{\mathrm{d}z} = \frac{\mathrm{d}}{\mathrm{d}z}\left(K\frac{\mathrm{d}U}{\mathrm{d}z}\right) = ac_{\mathrm{d}}U^2, \tag{17}$$

$$K = l^2\frac{\mathrm{d}U}{\mathrm{d}z}, \tag{18}$$

where τ (kg m^{-1} s^{-2}) is the vertical transfer of momentum, ρ (kg m^{-3}) is the air density, K (m^2 s^{-1}) is eddy diffusivity and l (m) is the mixing length.

Inoue (1963) assumed that l ($= l_{\rm h}$) and $ac_{\rm d}$ were constant within the canopy layer, and he obtained

$$\frac{U}{U_{\rm h}} = \frac{K}{K_{\rm h}} = \frac{u_*}{u_{\rm h*}} = \exp[\gamma(z-h)], \qquad z \le h, \tag{19}$$

where subscript h denotes the value at the canopy height $z = h$. The γ is already described in section 2 (Eq. (3)).

In the case of a dense and tall canopy, Kondo (1971) obtained the following equation from Eqs. (17), (18) and (19):

$$u_* = l_{\rm h}\gamma U, \qquad z \le h. \tag{20}$$

As taken by Inoue (1963), Kondo (1971) put

$$l_{\rm h} = k(h-d), \tag{21}$$

and assuming the continuity of u_* at $z = h$, the following equation was derived by substituting Eq. (20) and (21) into Eq. (1):

$$\ln\frac{h-d}{z_0} = \frac{1}{\gamma(h-d)}. \tag{22}$$

Kondo (1971) suggested that γ is the coefficient of momentum absorption by leaves and that $h - d$ is considered to be the depth proportional to the length at which the downward momentum disappears; thus, $\gamma(h - d)$ is assumed to be a non-dimensional constant.

B Continuity in shear stress and mixing length at the canopy top

If first-order closure (K-theory) is assumed for the airflow within and above the plant canopy then

$$\frac{\tau}{\rho} = K\frac{{\rm d}U}{{\rm d}z} = l^2\left|\frac{{\rm d}U}{{\rm d}z}\right|\frac{{\rm d}U}{{\rm d}z} \equiv u_*^2, \tag{23}$$

indicating that the continuity in the shear stress at the canopy top necessitates smoothness in the mean velocity profile. In other words, if U is differentiable at $z = h$, u_* is continuous for $z = h$. From this point of view, our theory in section 2 and the theory of Kondo (1971) in Appendix A are essentially equal. In addition, continuity in u_* (or τ) and ${\rm d}U/{\rm d}z$ guarantees continuity in the mixing length l at the canopy top. However, l is not smooth (differentiable) at the canopy top, because $l = k(z - d)$ above the canopy, whereas $l = l_{\rm h}$ =constant within the canopy.

From Eqs. (17) and (18), the momentum equation within the canopy in steady, horizontally homogeneous flow is (considering $l = l_{\rm h}$ =constant)

$$\frac{1}{\rho}\frac{{\rm d}\tau}{{\rm d}z} = \frac{\rm d}{{\rm d}z}\left(l_{\rm h}^2\left|\frac{{\rm d}U}{{\rm d}z}\right|\frac{{\rm d}U}{{\rm d}z}\right) = 2l_{\rm h}^2\left|\frac{{\rm d}U}{{\rm d}z}\right|\frac{{\rm d}^2U}{{\rm d}z^2} = ac_{\rm d}U^2, \tag{24}$$

which gives a non-linear second-order differential equation for U. The exponential profile of Inoue (1963), Eq. (2) in section 2 is the solution to Eq. (24), yielding

$$2l_{\rm h}^2\gamma^3\left\{U_{\rm h}\exp\left[\gamma(z-h)\right]\right\}^2 = ac_{\rm d}\left\{U_{\rm h}\exp\left[\gamma(z-h)\right]\right\}^2, \tag{25}$$

which allows the derivation of Eq. (3) in section 2. From Eq. (20), for $z = h$,

$$\gamma l_{\rm h} = \frac{u_*}{U_{\rm h}} = \beta. \tag{26}$$

Here β quantifies the mass flux through the canopy (Finnigan and Belcher, 2004). Substituting Eq. (26) into Eq. (3) then yields

$$l_{\rm h} = \frac{2\beta^3}{ac_{\rm d}}. \tag{27}$$

Equations (26) and (27) are related to Eq. (15). From the logarithmic law (Eq. (1)), the relationship between z_0 and $h - d$ is written as

$$z_0 = (h - d) \exp\left(-\frac{k}{\beta}\right), \tag{28}$$

and thus the continuity of the mixing length (without any smoothness constraints) leads to a linear relationship between d and $z0$, with a slope connected to the momentum extraction by the canopy. Because $l_\mathrm{h} = k(h - d)$, a continuous mixing length at the canopy top l_h automatically yields

$$d = h - \frac{l_\mathrm{h}}{k}, \tag{29}$$

$$z_0 = \frac{l_\mathrm{h}}{k} \exp\left(-\frac{k}{\beta}\right). \tag{30}$$

If $a = A/h =$ constant (where A is LAI), from Eq. (27),

$$\frac{d}{h} = 1 - \frac{2\beta^3}{kAc_\mathrm{d}}, \tag{31}$$

$$\frac{z_0}{h} = \frac{2\beta^3}{kAc_\mathrm{d}} \exp\left(-\frac{k}{\beta}\right), \tag{32}$$

which clearly shows how the canopy LAI (which is dependent on the tree LAI and the tree spacing) impacts the zero-plane displacement and roughness length.

References

Allen LH Jr (1968) Turbulence and wind speed spectra within a Japanese larch plantation. J Appl Meteorol 7:73–78

Bosveld FC (1997) Derivation of fluxes from profiles over a moderately homogeneous forest. Boundary-Layer Meteorol 84:289–327

Brunet Y, Irvine MR (2000) The control of coherent eddies in vegetation canopies: streamwise structure spacing, canopy share scale and atmospheric stability. Boundary-Layer Meteorol 94:139–163

Cellier P, Brunet Y (1992) Flux-gradient relationships above tall plant canopies. Agric For Meteorol 58:93–117

Cowan IR (1968) Mass, heat and momentum exchange between stands of plants and their atmospheric environment. Quart J Roy Meteorol Soc 94:523–544

de Bruin HAR, Moore CJ (1985) Zero-plane displacement and roughness length for tall vegetation, derived from a simple mass conservation hypothesis. Boundary-Layer Meteorol 31:39–49

Dolman AJ (1988) Estimates of roughness length and zero plane displacement for a foliated and non-foliated oak canopy. Agric For Meteorol 36:241–248

Dolman AJ, Moors EJ, Elbers JA (2002) The carbon uptake of a mid latitude pine forest growing on sandy soil. Agric For Meteorol 111:157–170

Finnigan JJ, Belcher SE (2004) Flow over a hill covered with a plant canopy. Quart J Roy Meteorol Soc 130:1–29

Garratt JR (1980) Surface influence upon vertical profiles in the atmospheric near-surface layer. Quart J Roy Meteorol Soc 106:803–819

Hall RL (2002) Aerodynamic resistance of coppiced poplar. Agric For Meteorol 114:83–102

Harman IN, Finnigan JJ (2007) A simple unified theory for flow in the canopy and roughness sublayer. Boundary-Layer Meteorol 123:339–363

Hicks BB, Hyson P, Moore CJ (1975) A study of eddy fluxed over a forest. J Appl Meteorol 14:58–66

Inoue E (1963) On the turbulent structure of airflow within crop canopies. J Meteorol Soc Jpn 41:317–326

Jacobs AFG, van Boxel JH (1988) Changes of the displacement height and roughness length of maize during a growing season. Agric For Meteorol 42:53–62
Kondo J (1971) Relationship between the roughness coefficient and other aerodynamic parameters. J Meteorol Soc Jpn 49:121–124
Legg BJ, Long IF (1975) Turbulent diffusion within a wheat canopy: II. Results and interpretation. Quart J Roy Meteorol Soc 101:611–628
Leonard RE, Federer CA (1973) Estimated and measured roughness parameters for a pine forest. J Appl Meteorol 12:302–307
Lo AK (1995) Determination of zero-plane displacement and roughness length of a forest canopy using profiles of limited height. Boundary-Layer Meteorol 75:381–402
Maki T (1975) Wind profile parameters of various canopies as influenced by wind velocity and stability. J Agric Meteorol 31:61–70 (in Japanese with English summary)
Maki T (1976) Aerodynamic characteristics of wind within and above a plant canopy — Interrelationship between aerodynamic parameters and plant canopy height —. Bull Natl Inst Agric Sci A23:1–67
Mölder M, Grelle A, Lindroth A, Halldin S (1999) Flux-profile relationships over a boreal forest — roughness sublayer corrections. Agric For Meteorol 98–99:645–658
Monteith JL, Unsworth M (1990) Principles of environmental physics, 2nd edn. Edward Arnold, London, 291 pp
Moore CJ (1974) A comparative study of forest and grassland micrometeorology. Ph.D. Thesis, The Flinders, University of South Australia, 237 pp
Nakai T, Kuwada T, Kodama Y, Ohta T, Maximov TC (2005) Comparison of aerodynamic characteristics among boreal, cool-temperate and warm-temperate forests. J Agric Meteorol 60(5):689–692
Nakai T, van der Molen MK, Gash JHC, Kodama Y (2006) Correction of sonic anemometry angle of attack errors. Agric Forest Meteorol 136:19–30
Nakai T, Sumida A, Daikoku K, Matsumoto K, van der Molen MK, Kodama Y, Kononov AV, Maximov TC, Dolman AJ, Yabuki H, Hara T, Ohta T (2008) Parameterisation of aerodynamic roughness over boreal, cool- and warm-temperate forests. Agric For Meteorol doi:10.1016/j.agrformet.2008.03.009
Raupach MR (1992) Drag and drag partition on rough surfaces. Boundary-Layer Meteorol 60:375–395
Raupach MR (1994) Simplified expressions for vegetation roughness length and zero-plane displacement as functions of canopy height and area index. Boundary-Layer Meteorol 71:211–216
Raupach MR, Finnigan JJ, Brunet Y (1996) Coherent eddies and turbulence in vegetation canopies: the mixing-layer analogy. Boundary-Layer Meteorol 78:351–382
Riggs DS, Guarnieri JA, Addelman S (1978) Fitting straight lines when both variables are subject to error. Life Sci 22:1305–1360
Rinne J, Tuovinen JP, Laurila T, Hakola H, Aurela M, Hypén H (2000) Measurements of hydrocarbon fluxes by a gradient method above a northern boreal forest. Agric For Meteorol 102:25–37
Rooney GG (2001) Comparison of upwind land use and roughness length measured in the urban boundary layer. Boundary-Layer Meteorol 100:469–486
Schaudt KJ (1998) A new method for estimating roughness parameters and evaluating the quality of observations. J Appl Meteorol 37:470–476
Schmid HP, Grimmond CSB, Cropley F, Offerle B, Su HB (2000) Measurements of CO_2 and energy fluxes over a mixed hardwood forest in the mid-western United States. Agric For Meteorol 103:357–374
Seginer J, Mulhearn PJ, Bradley ER, Finnigan JJ (1976) Turbulent flow in a model plant canopy. Boundary-Layer Meteorol 10:423–453
Shaw RH, Pereira AR (1982) Aerodynamic roughness of a plant canopy: a numerical experiment. Agric Meteorol 26:51–65
Shimano K (1997) Analysis of the relationship between DBH and crown projection area using a new model. J For Res 2:237–242
Tanner CB, Pelton WL (1960) Potential evapotranspiration estimates by the approximate energy balance of Penman. J Geophys Res 65:3391–3413

Thom AS (1971) Momentum absorption by vegetation. Quart J Roy Meteorol Soc 97:414–428

Thomas C, Foken T (2007) Organised motion in a tall spruce canopy: temporal scales, structure spacing and terrain effects. Boundary-Layer Meteorol 122:123–147

Turnipseed AA, Blanken PD, Anderson DE Monson RK (2002) Energy budget above a high-elevation subalpine forest in complex topography. Agric For Meteorol 110:177–201

Vesala T, Markkanen T, Palva L, Siivola E, Palmroth S, Hari P (2000) Effect of variations of PAR on CO_2 exchange estimation for Scots pine. Agric For Meteorol 100:337–347

Viswanadham Y, Molion LCB, Manzi LDA, Sá LDA, Silva Filho VP (1990) Micrometeorological measurements in amazon forest during GTE/ABLE 2A mission. J Geophys Res 95:13669–13682

Zobitz JM, Keener JP, Schnyder H, Bowling DR (2006) Sensitivity analysis and quantification of uncertainty for isotopic mixing relationships in carbon cycle research. Agric For Meteorol 136:56–75

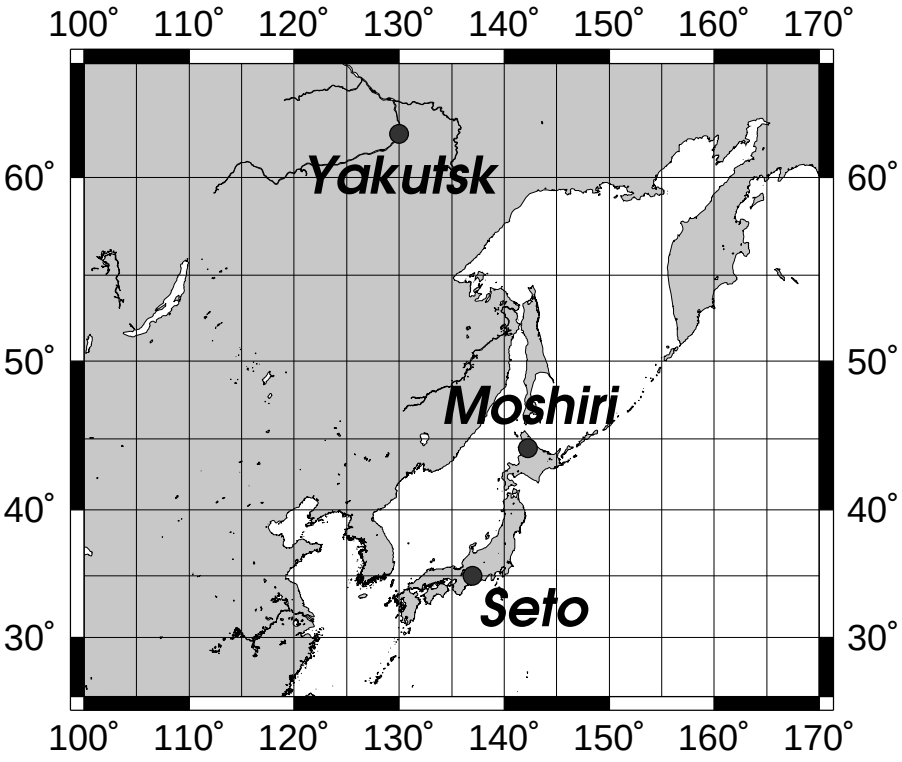


Fig. 1 Locations of Yakutsk, Moshiri and Seto, where our observations were conducted.

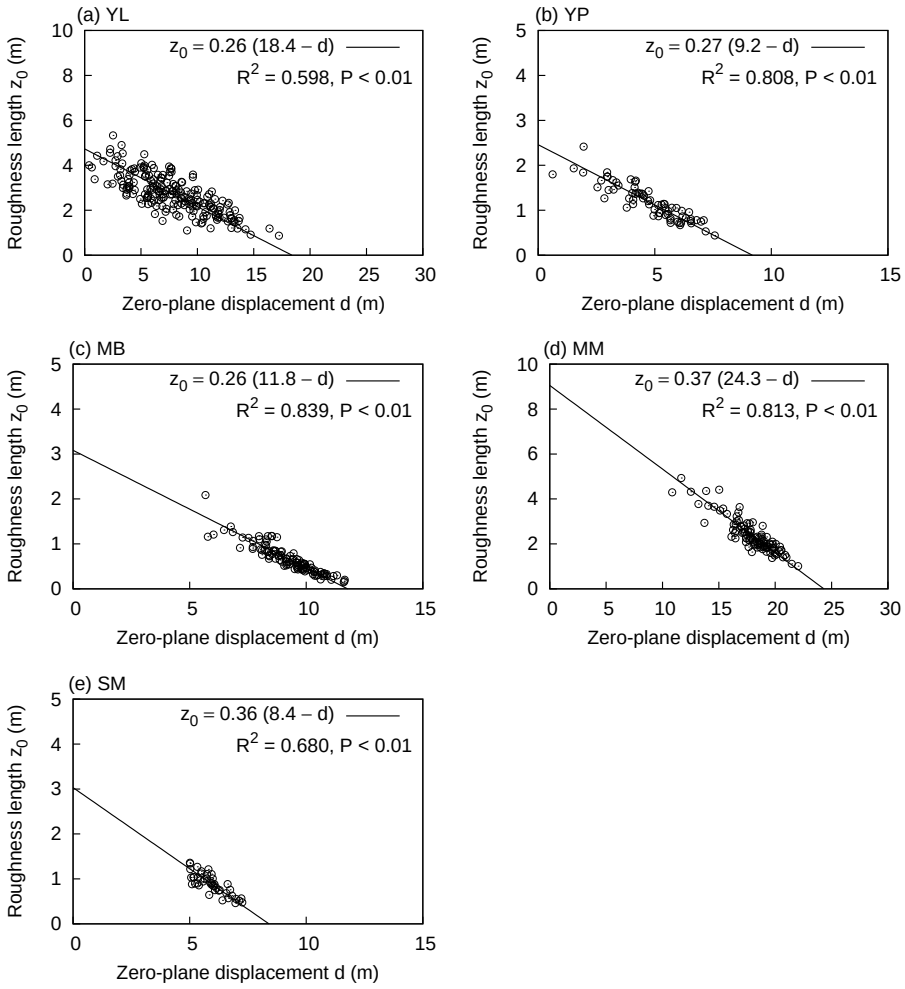


Fig. 2 Scatterplot of roughness length z_0 against zero-plane displacement d for the five forest sites. The regression lines of Model II are also described.

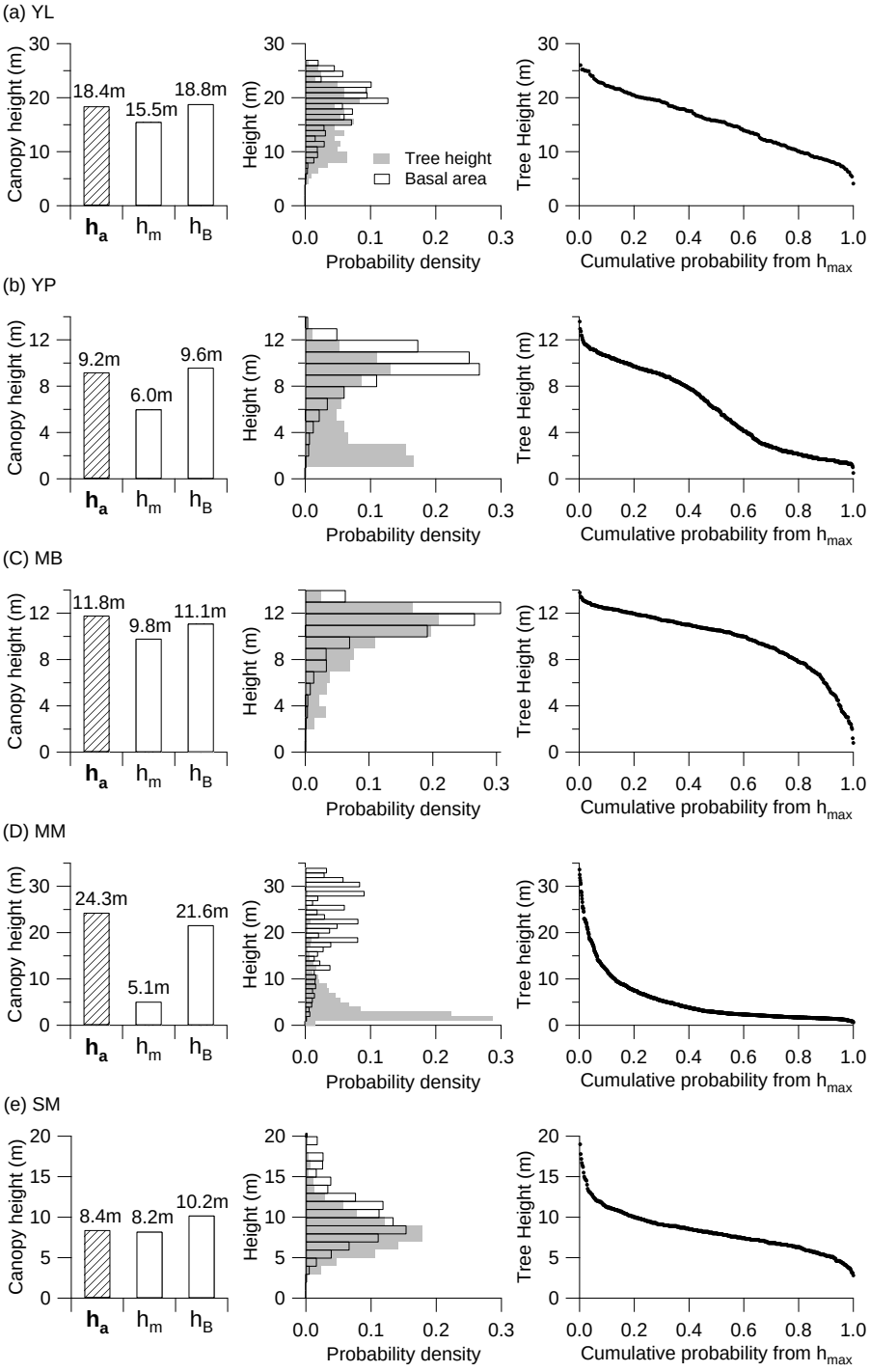


Fig. 3 Comparison of aerodynamic canopy height h_{a} with various values calculated from stand inventory data. The left-hand plot is the comparison of h_{a} with mean tree height h_{m} and weighted mean canopy height with basal area h_{B}. The middle plot is the vertical distribution of the frequency in tree height h and basal area for each 1-m tree height class, given as probability densities. The right-hand plot shows the cumulative probability of h from the maximum tree height h_{max}.

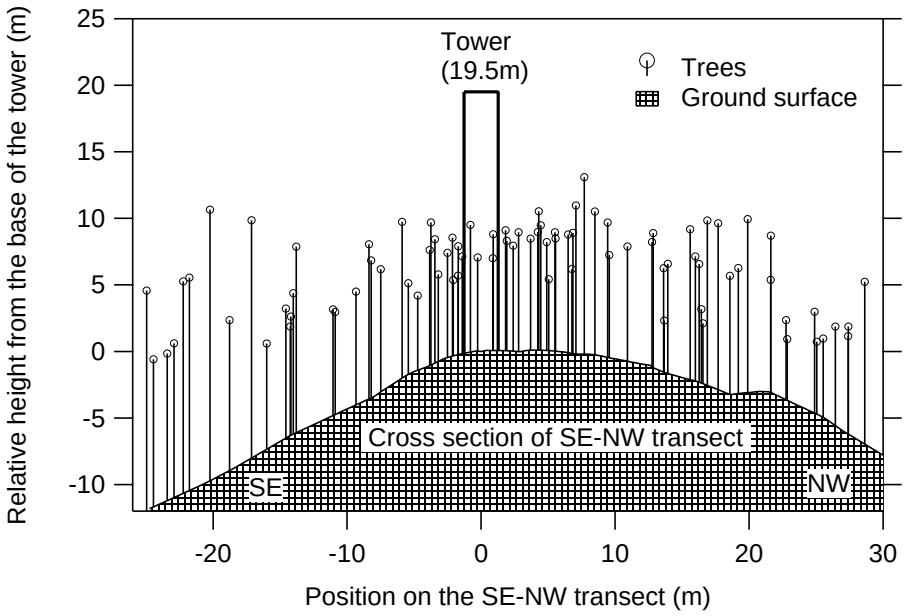


Fig. 4 Cross section of the transect from southeast to northwest through the meteorological tower in the SM site. The elevation is shown as relative height from the base of the tower. The plotted trees are the samples located within the belt of 10 m width along the transect.

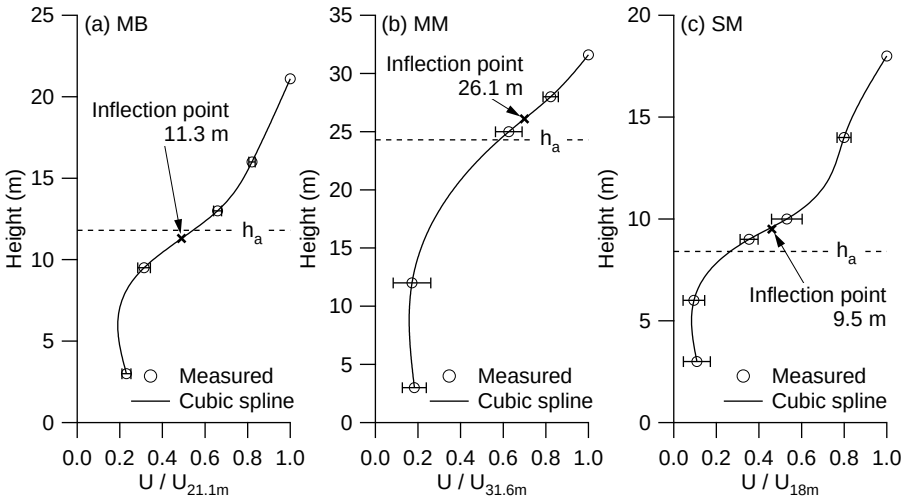


Fig. 5 Vertical profile of relative wind speeds normalised to the wind speed at the top of the tower, and a cubic spline interpolation of its mean values at the MB, MM and SM sites. Open circles and error bars indicate the mean value and standard deviation, respectively, of the relative wind speed. Inflection points of these cubic spline functions and our results for aerodynamic canopy height h_{a} are also described.

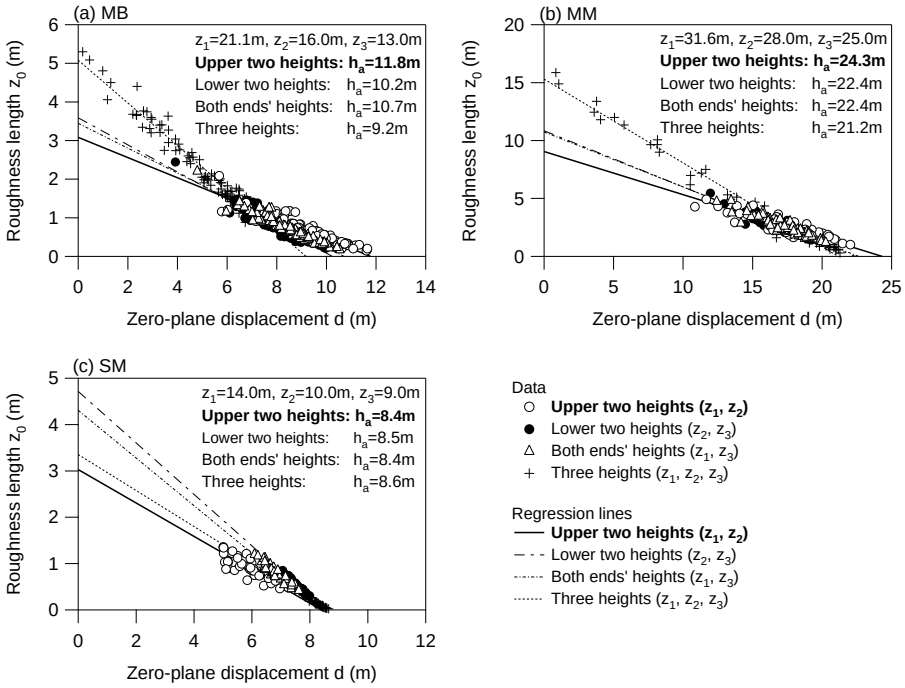


Fig. 6 Scatterplot of roughness length z_0 against zero-plane displacement d at sites MB (a), MM (b) and SM (c) calculated from the wind speeds at the two upper and the two lower heights, both ends, and three heights. The resulting aerodynamic canopy height h_a values are also listed. The results from the upper two heights are the same as those in Fig. 2.

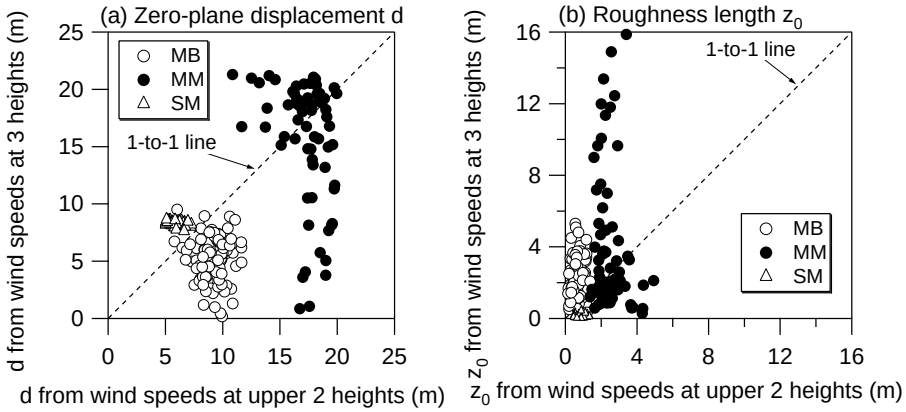


Fig. 7 Scatterplot of zero-plane displacement d (a) and roughness length z_0 (b) calculated from the wind profile at three heights against those values derived from wind speeds at the upper two heights via Eqs. (9) and (10).

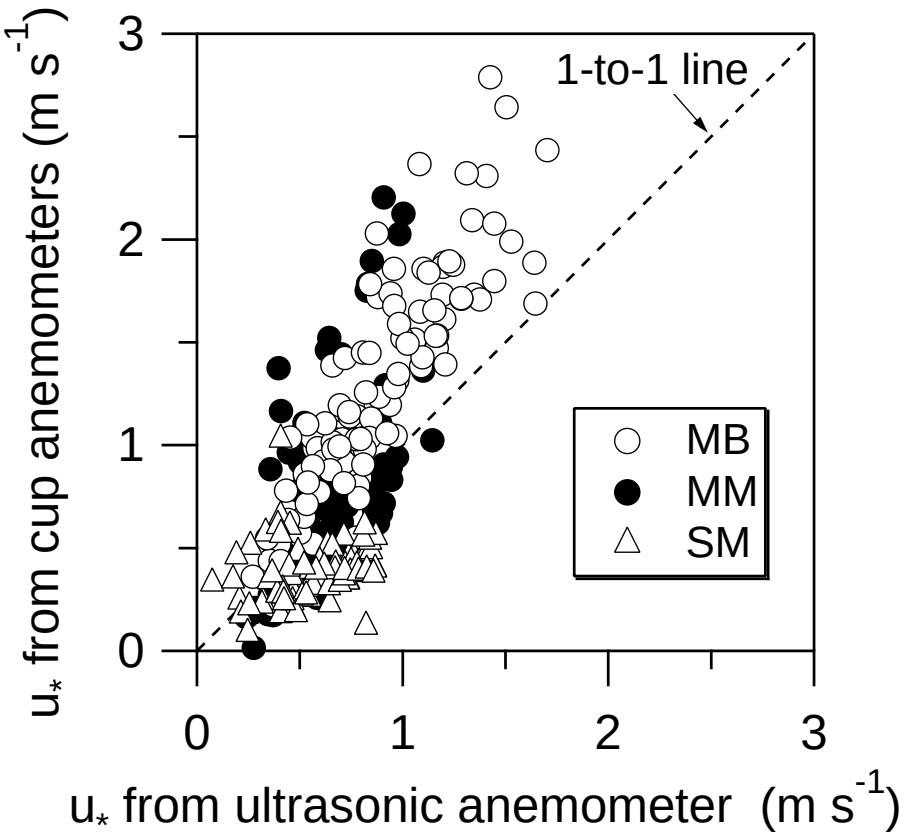


Fig. 8 Scatterplot of friction velocity u_* calculated from wind speeds measured by cup anemometers at three heights against that directly measured by an ultrasonic anemometer.

Table 1 Location, stand characteristics and measurement conditions of the five observation sites.

Site	YL	YP	MB	MM	SM
Latitude	62° 15′ 18″ N	62° 14′ 29″ N	44° 23′ 03″ N	44° 19′ 19″N	35° 15′ 29″ N
Longitude	129° 37′ 08″ E	129° 39′ 02″ E	142° 19′ 07″ E	142° 15′ 41″E	137° 04′ 54″ E
Altitude (m ASL)	220	220	585	340	205
Stand density (stands ha^{-1})	840	2660	4384	2585	1828
Maximum tree height h_{max} (m)	26.0	13.6	13.8	33.6	19.0
Mean tree height h_m (m)	15.5	6.0	9.8	5.1	8.2
Standard deviation of tree height σ_h (m)	5.2	3.5	2.6	5.3	2.5
Height of ultrasonic anemometer z_e (m)	32.0	18.2	21.1	31.6	19.5
Height of cup anemometer z_1 (m)	32.0	18.2	21.1	31.6	14.0
Height of cup anemometer z_2 (m)	27.0	13.8	16.0	28.0	10.0
Wind direction (clockwise from north)	−30° to 30°	0° to 60°	255° to 270°	255° to 285°	290° to 320°
Area of forest survey plot	50m×50m	50m×50m	20m×30m×2	40m×100m	50m×50m
Dominant tree species	*Larix cajanderi*	*Pinus sylvestris*	*Betula ermanii*	*Picea glehnii*, *Betula platyphylla* var. *japonica*	*Quercus serrata*, *Ilex pedunculosa*

Table 2 The coefficient λ in previous studies.

Reference	λ	Condition
Moore (1974)	0.26 $\pm$0.07	105 published d, z_0 and h data
Seginer (1974)	0.37	Canopy wind model of Inoue (1963) and an observation by Kondo (1971)
Legg and Long (1975)	0.31	Wheat crop
Maki (1975, 1976)	0.48 $\pm$ 0.02	Teosinte
	0.56 $\pm$ 0.02	Corn
	0.27 $\pm$ 0.03	Sorgo
	0.47	Japanese larch (Allen, 1968)
	0.56 $\pm$ 0.05	Glass rod model canopy (wind tunnel)
Hicks *et al.* (1975)	0.36	Pine forest (*Pinus radiata*)
Shaw and Pereira (1982)	0.29	Second-order closure model results (plot through origin)
De Bruin and Moore (1985)	0.22	Pine forest (*Pinus sylvestris*)
Jacobs and van Boxel (1985)	0.25	forage maize (*Zea mays* L., Vivia)

Table 3 Canopy height h (m), zero-plane displacement d (m) and roughness length z_0 (m) from previous studies, and calculated coefficient λ and aerodynamic canopy height h_a (m). h_a from these data was estimated for $\lambda = 0.32 \pm 0.12$, that is, the mean value and standard deviation of calculated λ.

Reference	h (m)	d (m)	z_0 (m)	λ	h_a (m) $\lambda = 0.32(\pm 0.12)$	Forest condition
Allen (1968)	10.4	6.34	0.82	0.20	8.9 (8.2 – 10.4)	Japanese larch
Bosveld (1997)	18.0	12.5	2.0	0.36	18.8 (17.0 – 22.5)	Douglas fir
de Bruin and Moore (1985)	18.5	11.5	1.37	0.20	15.8 (14.6 – 18.4)	European red pine (*Pinus sylvestris*)
Dolman (1986)	9.6	7.2	1.0	0.42	10.3 (9.5 – 12.2)	Oak (foliated)
	9.6	5.5	0.9	0.22	8.3 (7.5 – 10.0)	Oak (non-foliated)
Dolman et al(2002)	15.1	9.9	2.05	0.39	16.3 (14.6 – 20.2)	Scots pine
Hall (2002)	6.2	4.89	0.36	0.28	6.0 (5.7 – 6.7)	Poplar
Hicks et al (1975)	12.4	9.8	0.32	0.12	10.8 (10.5 – 11.4)	Radiata pine (*Pinus radiata*) (May)
	13.3	11.9	0.54	0.39	13.6 (13.1 – 14.6)	Radiata pine (*Pinus radiata*) (October)
Leonard and Federer (1973)	14.9	9.6	1.0	0.19	12.7 (11.9 – 14.6)	Red pine
Lo (1995)	18.5	12.7	0.97	0.17	15.7 (14.9 – 17.5)	Aspen, Red maple
Rinne et al (2000)	13.0	8.7	1.03	0.24	11.9 (11.0 – 13.9)	Mountain birch , Siberian spruce and Scots pine
Schmid et al (2000)	26.0	20.8	2.1	0.40	27.4 (25.6 – 31.3)	Sugar maple, Tulip poplar, Sassafras, White oak, Black oak
Turnipseed et al (2002)	11.4	7.8	1.62	0.45	12.9 (11.5 – 15.9)	Subalpine fir, Engelmann spruce, Lodgepole pine
Vesala et al (2000)	13.0	6.0	0.8	0.11	8.5 (7.8 – 10.0)	Scots pine
Viswanadham et al (1990)	35.0	30.9	2.2	0.54	37.8 (35.9 – 41.9)	Leguminosae, Sapotaceae
Yang and Friedl (2003)	11.2	7.4	1.65	0.43	12.6 (11.2 – 15.7)	Old black spruce
	16.2	11.0	1.81	0.35	16.7 (15.1 – 20.1)	Old jackpine
	13.5	9.2	1.4	0.33	13.6 (12.4 – 16.2)	Old black spruce

Certificate of English revision

The English in this document has been checked by at least two professional editors, both native speakers of English. For a certificate, see:

http://www.textcheck.com/cgi-bin/certificate.cgi?id=G0mDWE